


## ORIGINAL ARTICLE

# Hepatic and abdominal adiposity in type 2 diabetes as assessed with machine learning on computed tomography scans

Richard H. Tran BA<sup>1,2</sup>  | Pavan Raghupathy BS<sup>1</sup> | Mohamad Hazim BA<sup>1</sup> | Elizabeth Thompson PhD<sup>1</sup> | Sophia Swago PhD<sup>1</sup> | Abhijit Bhattaru BS<sup>1</sup> | Matthew MacLean MD<sup>1</sup> | Jeffrey T. Duda PhD<sup>1</sup> | James Gee PhD<sup>1</sup> | Charles Kahn Jr. MD<sup>1</sup> | Daniel J. Rader MD<sup>3</sup> | Arijitt Borthakur PhD<sup>1,4</sup> | Walter R. Witschey PhD<sup>1</sup> | Hersh Sagreiya MD<sup>1</sup>

<sup>1</sup>Department of Radiology, Perelman School of Medicine, University of Pennsylvania, Philadelphia, Pennsylvania, USA

<sup>2</sup>Department of Medicine, University of Massachusetts Chan Medical School, Worcester, Massachusetts, USA

<sup>3</sup>Department of Genetics, Perelman School of Medicine, University of Pennsylvania, Philadelphia, Pennsylvania, USA

<sup>4</sup>Leonard Davis Institute of Health Economics, University of Pennsylvania, Philadelphia, Pennsylvania, USA

## Correspondence

Hersh Sagreiya, Division of Abdominal Imaging, Department of Radiology, Hospital of the University of Pennsylvania, 3400 Spruce Street, Philadelphia, PA 19104, USA.  
Email: [hersh.sagreiya@penmedicine.upenn.edu](mailto:hersh.sagreiya@penmedicine.upenn.edu)

## Funding information

National Center for Advancing Translational Sciences, Grant/Award Number: UL1TR001878; Institute for Translational Medicine and Therapeutics Transdisciplinary Program in Translational Medicine and Therapeutics; Sarnoff Cardiovascular Research Foundation Sarnoff Fellowship Program; Radiological Society of North America, Grant/Award Number: #RSCH2028; National Heart, Lung, and Blood Institute, Grant/Award Numbers: R01HL169378, R01HL171709; National Institute of Biomedical Imaging and Bioengineering, Grant/Award Numbers: P41EB029460, R21EB036734; NIH Office of the Director, Grant/Award Number: OT2OD038048

## Abstract

**Aims:** The combined assessment of multiple abdominal imaging traits in relation to type 2 diabetes remains incompletely characterised. The study examines these relationships on computed tomography (CT) scans from a large-scale, racially diverse, disease-focused medical biobank.

**Materials and Methods:** Deep learning algorithms were applied to patients with abdominal CT scans in the Penn Medicine BioBank to quantify image-derived phenotypes, including spleen-hepatic attenuation difference (SHAD) for hepatic steatosis (HS), liver and spleen volumes (SV), abdominal visceral and subcutaneous adipose tissue (VAT and SAT, respectively) and visceral-to-subcutaneous ratio (VSR). One thousand five hundred and ninety-four patients (62 years, 49.4% male, 59.3% White), comprising 950 nondiabetics and 644 diabetics, were included in analysis with diabetes status determined by a 6.5% haemoglobin A1c cutoff.

**Results:** Diabetic patients had greater HS (SHAD  $-4.49$  vs.  $-6.88$  Hounsfield units,  $p = 1.34 \times 10^{-8}$ ), steatosis prevalence (41.8% vs. 27.7%,  $p = 4.85 \times 10^{-9}$ ) and VSR (0.62 vs. 0.55,  $p = 1.69 \times 10^{-3}$ ) than nondiabetics. In multivariate analyses adjusting for age, sex, race and body mass index (BMI), diabetes was independently associated with SHAD (odds ratios [OR] 1.04, 95% confidence interval [1.02–1.05]), SV (OR 4.53 [1.89–10.99]) and VSR (OR 2.87, [1.96–4.20]). Combined regression

Richard H. Tran and Pavan Raghupathy contributed equally to the manuscript and will be considered co-first authors.

Parts of this paper were presented as an abstract at the 2023 American Roentgen Ray Society Annual Meeting in Honolulu, HI, USA. The citation is noted below: Tran, R., Raghupathy, P., MacLean, M., Gee, J., Rader, D.J., Witschey, W.R., Sagreiya, H.: Hepatic steatosis in the diabetic population as assessed by using machine learning on CT scans. American Roentgen Ray Society Annual Meeting, April 2023, Honolulu, HI.

This is an open access article under the terms of the [Creative Commons Attribution](https://creativecommons.org/licenses/by/4.0/) License, which permits use, distribution and reproduction in any medium, provided the original work is properly cited.

© 2026 The Author(s). *Diabetes, Obesity and Metabolism* published by John Wiley & Sons Ltd.

analysis showed no relationship between splenomegaly and type 2 diabetes once controlling for hepatic factors (OR 1.08, [0.95–1.23]), but uncovered a stronger VSR correlation (OR 1.40, [1.20–1.63]) than BMI (OR 1.14, [1.01–1.29]).

**Conclusions:** Hepatic steatosis, hepatomegaly and visceral adiposity on CT are associated with type 2 diabetes. Hepatic changes may influence spleen size effects on diabetes. VSR can serve as an alternative to traditional obesity metrics to accurately reflect diabetes risk.

#### KEYWORDS

abdominal adiposity, artificial intelligence, computed tomography, hepatic steatosis, machine learning, subcutaneous adipose tissue, type 2 diabetes, visceral adipose tissue

## 1 | INTRODUCTION

Diabetes mellitus is projected to impact over 780 million people globally by 2045.<sup>1,2</sup> Despite its prevalence, the disease is typically underdiagnosed and detected at later stages, leading to missed opportunities for early intervention that can prevent serious associated cardiometabolic diseases.<sup>3–5</sup> Imaging represents a potential opportunistic screening tool, whereby information obtained during routine or unrelated clinical assessments can be leveraged to determine the presence of type 2 diabetes and its associated risk factors.<sup>6</sup>

With over 85 million computed tomography (CT) scans performed in the United States each year, there is opportunity to harness such data to identify patients with type 2 diabetes.<sup>7</sup> The advancement of machine learning in radiology has allowed for efficient and rapid analysis of substantial amounts of data, with applications seen in the assessment of stroke, osteoporosis and sarcopenia on CT scans.<sup>8–11</sup> These approaches allow for extraction and calculations of quantitative imaging measurements, or image-derived phenotypes (IDPs), from radiological scans to explore novel disease associations, expanding our ability to perform phenotypic assessments as part of clinical care and improve clinical decision making.<sup>11–13</sup> As IDPs are automatically quantified and established at the time of the study, their use presents no additional risk to the patient and provides an opportunity to detect findings that could be missed by radiologists, especially given the large volume of studies they typically read.

Prior studies have independently quantified abdominal IDPs, including HS through the spleen-hepatic attenuation difference (SHAD), central adiposity which includes visceral adipose tissue (VAT) located between organs and subcutaneous adipose tissue (SAT) located peripherally under the skin, liver organ size, as well as evaluated their relationship with type 2 diabetes on CT scans.<sup>13–18</sup> However, an integrated assessment of these abdominal imaging phenotypes remains incompletely characterised. Moreover, there has been limited attention to spleen size and its relationship to type 2 diabetes, even though splenic metrics are routinely used to calculate HS.<sup>14,16,19,20</sup> A comprehensive approach may clarify interrelationships among these abdominal IDP values and improve type 2 diabetes risk stratification beyond individual parameters. CT scans are particularly well-suited for such large-scale cumulative analyses as alternative

non-invasive diagnostic methods such as magnetic resonance imaging are expensive and not as cost-effective, while ultrasound demonstrates inter-reader variability in qualitative steatosis assessment.<sup>21–24</sup>

In this study, we leveraged body composition analysis to uncover imaging markers of metabolic dysfunction in the diabetic population. We utilised electronic health record (EHR) data from participants enrolled in the Penn Medicine BioBank (PMBB) to identify patients with non-contrast abdominal CT scans and an associated haemoglobin A1c (HbA1c) value of  $\geq 6.5\%$  as a diabetes diagnosis. Using machine learning methods, we automated the analysis of certain abdominal IDPs, including SHAD, liver volume (LV), spleen volume (SV), abdominal VAT, abdominal SAT and visceral-to-subcutaneous fat ratio (VSR). We aim to quantify the differences in these IDPs between individuals with and without type 2 diabetes, as well as explore the combined associations of HS, abdominal fat distribution and hepatosplenic organ size with the presence of type 2 diabetes.

## 2 | MATERIALS AND METHODS

### 2.1 | Institution

This study utilised data from the PMBB, a biomedical database consisting of advanced imaging, biological samples and other EHR data from over 250 000 patients within the University of Pennsylvania Health System, a multi-hospital network headquartered in Philadelphia, PA. All enrolled patients provided informed consent for researchers to access their EHR.

### 2.2 | Study cohort imaging data

From 1998 to 2019, 13 503 patients were identified that received abdominal and pelvic CT scans designated by the appropriate Current Procedural Terminology codes (Figure S1). Nine thousand one hundred and forty-nine PMBB patients had abdominal CT scans that yielded IDP values for hepatic and abdominal adiposity based on our deep learning algorithm (discussed below). To associate a single SHAD value to each patient, we first selected the image series within each

CT examination that had the SHAD value closest to the median SHAD of that entire exam. Of note, a patient can have multiple CT exams on different dates, and each CT exam has multiple series. Then, we grouped the data by PMBB identification number, which identified each unique patient, and selected the study that had the greatest SHAD value per patient. This was done in order to ensure the maximum degree of hepatic steatosis was captured for each patient. Patients with SHAD values within  $-30$  Hounsfield units (HU) and  $30$  HU were included. Certain exclusion criteria were applied

sequentially to obtain the patient population of interest (Figure 1). In brief, missing and extraneous IDPs were removed. Patients with missing age values were removed. We used mapped phecodes, which are disease phenotypes derived from the International Classification of Diseases, Ninth Revision (ICD-9) (<https://www.phewascatalog.org/phecodes>) to apply exclusionary criteria for certain diseases (Figure S2).<sup>25</sup> Additionally, those without HbA1c values within a year of the CT study date were excluded from the analysis. For patients with multiple HbA1c measurements within the 1-year window, the

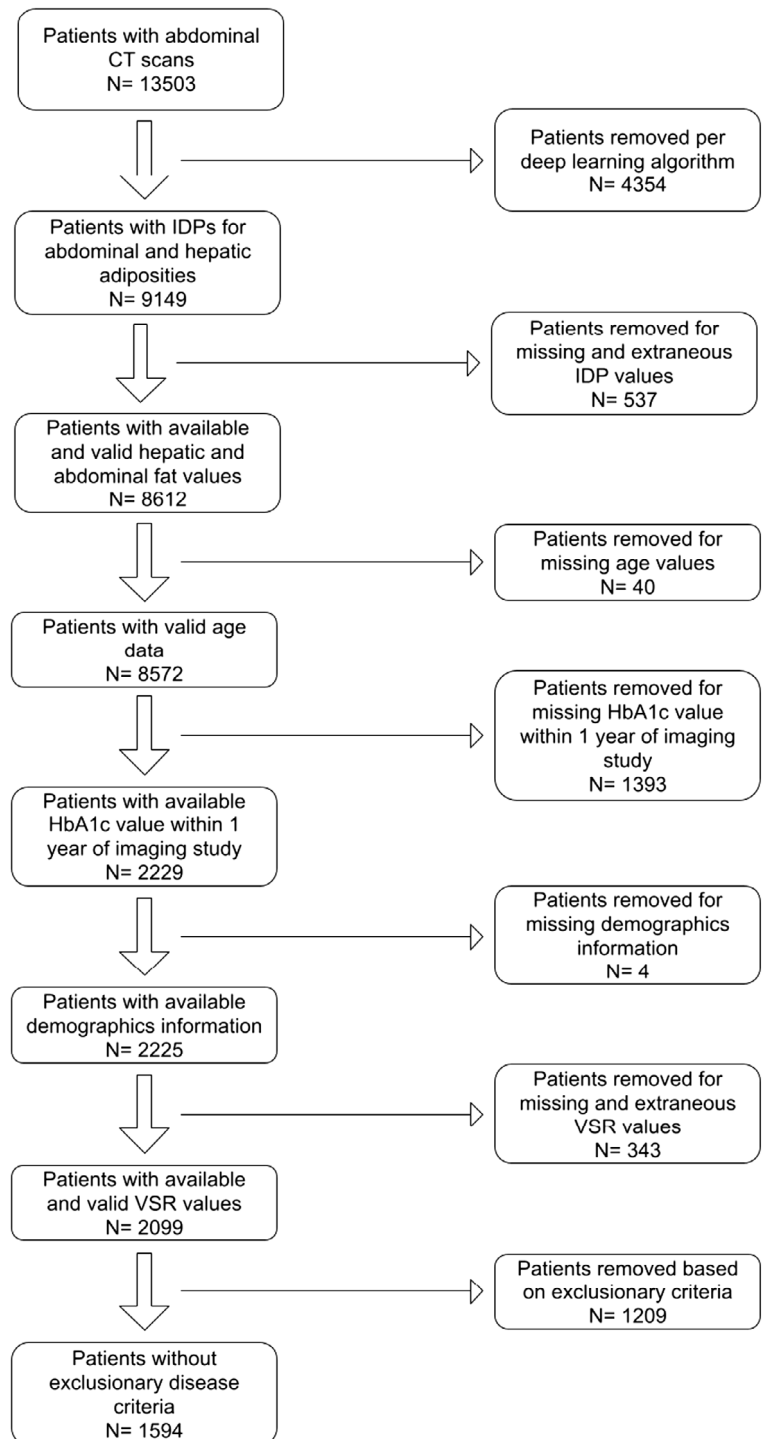


**FIGURE 1** Patient flowchart. Number of patients in Penn Medicine BioBank with available quantified image derived phenotypes related to hepatic and abdominal fat. Patients with applicable phecodes (alcohol use disorder, hepatitis and end-stage liver disease) were excluded from the final analysis. CT, computed tomography; HbA1c, haemoglobin A1c; IDPs, image-derived phenotypes; VSR, visceral-to-subcutaneous ratio.

value closest in time to the CT study was used. Patients with missing demographic information (race, body mass index [BMI] and sex) were excluded. VSR was calculated by dividing VAT by SAT. Patients without VSR or outlier values were excluded. Patients with alcohol use disorder, alcohol-related liver disease, end-stage liver disease and viral hepatitis phecodes were excluded to remove potential confounders. The final cohort comprised 1594 patients and data were collected for age, sex, race/ethnicity, BMI, HbA1c and medication use (Figure 1). Type 2 diabetes status was defined based on HbA1c values  $\geq 6.5\%$  obtained within 1 year of the imaging study. Race and ethnicity were included in the analysis to account for population-level differences in BMI cutoffs for obesity.<sup>26,27</sup> Patients with their ethnicity classified as Hispanic or Latino were considered as another race cohort, independent of race. Medication use was summarised descriptively to characterise the cohort.

### 2.3 | Machine learning algorithm for adipose quantification

A well-defined deep learning method that our group previously developed (Dice Score coefficients ranging from 0.92 to 1.00) was applied for the segmentation and quantification of liver fat, liver and splenic volume and abdominal adipose tissue.<sup>13,15,28,29</sup> In short, axial abdominal CT scans that had high-pass filter kernel resolutions or those with image slice thickness  $< 2$  mm were excluded to eliminate noise. Imaging studies with  $< 10$  slices were excluded to avoid incomplete studies. The applied deep learning method consists of three convolutional

neural networks (CNNs) (Figure 2): CNN<sub>1</sub> identified non-contrast CTs, as contrast bolus affects peak splenic and hepatic attenuation in a time-dependent manner.<sup>30</sup> CNN<sub>2</sub> defined certain axial slices as the abdominal compartment boundaries between the inferior thoracic cavity and L5 vertebrae. Lastly, fully automated segmentation of the liver (CNN<sub>3A</sub>), spleen (CNN<sub>3B</sub>) and delineation of abdominal SAT and VAT were conducted (CNN<sub>3C</sub>). Liver, spleen, and abdominal SAT and VAT cross-sectional areas were measured on each axial slice, with their respective total volumes computed as the sum across slices within the abdominal compartment, leading to LV, SV, abdominal VAT volume and abdominal SAT volume. Liver and spleen mean attenuation values (LMA and SMA, respectively) were determined from the imaging scans to calculate SHAD, spleen attenuation minus liver attenuation. A greater or more positive value for SHAD corresponds with increased liver adiposity. We delineate HS through either a LMA  $< 40$  HU or a SHAD  $\geq -1$  HU. This value for SHAD has previously been found to represent the cutoff for mild HS, as the typical SHAD cutoff of 10 HU is actually more concordant with the cutoff for moderate–severe HS.<sup>21,31</sup>

### 2.4 | Statistical analysis

All statistical tests were done using R (R Core Team, version 4.3.1; Foundation for Statistical Computing, Vienna, Austria). Patients were considered as diabetic if their HbA1c level was greater than or equal to 6.5%, while those that fell below this threshold were considered nondiabetic. Demographic information was collected. Moreover, IDPs

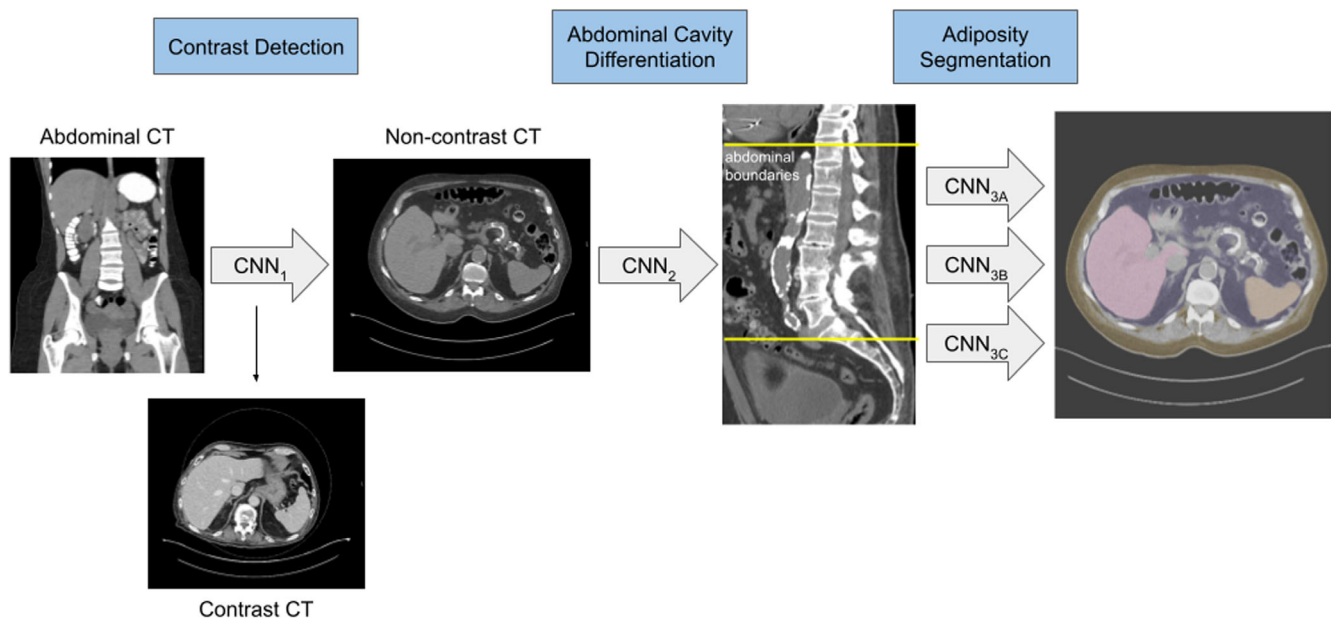


**FIGURE 2** Deep learning method for the segmentation and quantification of hepatic and abdominal adiposity. CNN<sub>1</sub> identified non-contrast from contrast computed tomography (CT) scans. CNN<sub>2</sub> delineated the boundaries of the abdominal compartment. The third convolutional neural network (CNN) simultaneously segmented the liver (CNN<sub>3A</sub>) (in pink), spleen (CNN<sub>3B</sub>) (in orange), and characterised visceral adipose tissue area (in purple) from subcutaneous adipose tissue area (in yellow) (CNN<sub>3C</sub>). Hepatic steatosis was diagnosed if spleen-hepatic attenuation difference was greater than  $-1$  Hounsfield unit (HU) or liver mean attenuation was less than 40 HU.

from abdominal CT, such as LMA, SMA, SHAD, VAT, SAT and VSR, were determined. Hepatic steatosis prevalence in each cohort was calculated. Differences in categorical variables (sex and race) between cohorts were determined using the chi-square test of independence. Differences in continuous variables (age, BMI, LMA, SHAD, VAT, SAT, VSR, HS prevalence) were determined using a two-sided Wilcoxon rank-sum test. Boxplots were created to compare IDP values with diabetes presence, stratified by sex. Multivariate regression analyses were performed for the presence of type 2 diabetes, looking independently at IDPs (SHAD, LV, SV, VAT, SAT and VSR). The model shown below (Model 1) represents the six iterations of the regression analyses performed with each IDP, controlling for sex, age, BMI and race. Odds ratios (ORs) were calculated from the multivariate analyses, including the 95% confidence interval (CI). *p*-Values were adjusted with Benjamini–Hochberg false discovery rate (BH-FDR) correction to reduce type 1 error with the statistical significance threshold of  $p < 0.05$ .

$$\text{Model 1: } \log \frac{p(\text{DIS} = 1)}{p(\text{DIS} = 0)} = \text{SEX} + \text{AGE} + \text{BMI} + \text{RACE} + \text{IDP}.$$

Additionally, regression analysis was performed using a second model (Model 2), which combined the previously described IDPs into

a single multivariable model that can assess whether individual phenotypes were independently associated with diabetes after accounting for correlations among imaging measures. To allow for comparison of effect sizes across the IDPs with different units, continuous variables were standardised to a mean of zero and a standard deviation of one for analysis in the combined multivariable model. In this model, standardised OR represents the change in odds of diabetes presence per one standard deviation increase in each continuous variable. VSR was used in the model in place of abdominal VAT and SAT to reduce multicollinearity while preserving information on the association between fat distribution and diabetes presence.

$$\text{Model 2: } \log \frac{p(\text{DIS} = 1)}{p(\text{DIS} = 0)} = \text{SEX} + \text{AGE} + \text{BMI} + \text{RACE} + \text{SHAD} + \text{SV} + \text{LV} + \text{VSR}.$$

### 3 | RESULTS

#### 3.1 | Patient cohort

Patients were dichotomised by the HbA1c threshold of 6.5% (Table 1). No statistical significance was found between the

**TABLE 1** Patient cohort demographics.

Total (n = 1594)	Nondiabetic (n = 950)	T2DM (n = 644)	<i>p</i> -Value
Age (years)	62 [52, 70]	62 [53, 69]	0.99
Sex (n [%])			0.38
Male	461 (48.5)	327 (50.8)	
Female	489 (51.5)	317 (49.2)	
Race (n [%])			$4.02 \times 10^{-7}$
White	618 (65.0)	327 (50.8)	
Black	268 (28.2)	266 (41.3)	
Asian/PI	18 (1.9)	20 (3.1)	
Hispanic/Latino	22 (2.3)	16 (2.5)	
Other	24 (2.5)	15 (2.3)	
BMI (kg/m <sup>2</sup> )	29.3 [25.4, 34.7]	31.2 [27.2, 36.5]	$3.15 \times 10^{-7}$
HbA1c (%)	5.7 [5.4, 6.0]	7.6 [6.9, 9.1]	$<2.2 \times 10^{-16}$
Medications (n [%])			
Metformin	144 (15.2)	282 (43.8)	$<2.2 \times 10^{-16}$
Sulfonylureas	44 (4.6)	134 (20.8)	$<2.2 \times 10^{-16}$
GLP-1 agonists	29 (3.1)	73 (11.3)	$6.75 \times 10^{-11}$
SGLT2 inhibitors	7 (0.7)	35 (5.4)	$2.31 \times 10^{-8}$
TZDs	13 (1.4)	22 (3.4)	$1.03 \times 10^{-2}$

Note: The demographic characteristics of included patients from the Penn Medicine BioBank. Age, sex, HbA1c are arranged as median [Q1, Q3]. Sex and race are organised as sample size (percentage).

*p*-Values for continuous variables (age, BMI) were calculated using a Wilcoxon rank-sum test and for categorical variables (sex, race) using a chi-square test of independence to determine statistically significant differences between the ‘Nondiabetic’ and ‘T2DM’ groups.

Abbreviations: BMI, body mass index; GLP-1, glucagon-like peptide-1; HbA1c, haemoglobin A1c; PI, Pacific Islander; SGLT2, sodium-glucose cotransporter 2; T2DM, type 2 diabetes mellitus; TZD, thiazolidinediones.

nondiabetic and diabetic cohorts for age (62 vs. 62 years,  $p = 0.99$ ) or sex (48.5% male vs. 50.8% male,  $p = 0.38$ ). The diabetic cohort exhibited greater racial diversity; the percentage of Black patients was greater for the type 2 diabetes group than the nondiabetic counterpart (41.3% vs. 28.2%,  $p = 4.02 \times 10^{-7}$ ), while the percentage of White patients was lower for the type 2 diabetes group (50.8% vs. 65.0%). Patients with type 2 diabetes had a higher BMI than patients without diabetes (31.2 vs. 29.3 kg/m<sup>2</sup>,  $p = 3.15 \times 10^{-7}$ ). Patients with type 2 diabetes also had a higher median HbA1c value than patients without diabetes (5.7% vs. 7.6%,  $p < 2.2 \times 10^{-16}$ ). Additionally, proportions of patients using select medication classes were found to be significantly higher in diabetic patients: metformin (43.8% vs. 15.2%,  $p < 2.2 \times 10^{-16}$ ); sulfonylureas (20.8% vs. 4.6%,  $p < 2.2 \times 10^{-16}$ ); glucagon-like peptide-1 agonists (11.3% vs. 3.1%,  $p = 6.75 \times 10^{-11}$ ); sodium-glucose cotransporter 2 inhibitors (5.4% vs. 0.7%,  $p = 2.31 \times 10^{-8}$ ); and thiazolidinediones (3.4% vs. 1.4%,  $p = 1.03 \times 10^{-2}$ ).

Hepatic and abdominal IDPs were quantified and stratified based on type 2 diabetes diagnosis (Table 2). Both SV (0.19 L vs. 0.18 L,  $p = 2.67 \times 10^{-2}$ ) and LV (1.74 L vs. 1.58 L,  $p = 5.02 \times 10^{-8}$ ) were larger in the type 2 diabetes patient cohort than in the nondiabetes cohort. LMA for diabetics was lower than for nondiabetics (47.0 vs. 50.9 HU,  $p = 1.36 \times 10^{-10}$ ), as well as SMA (43.2 vs. 44.3 HU,  $p = 2.67 \times 10^{-2}$ ). SHAD was greater in diabetics (−4.49 vs. −6.88 HU,  $p = 1.34 \times 10^{-8}$ ). The presence of HS was greater in the diabetic cohort (41.8% vs. 27.7%,  $p = 4.85 \times 10^{-9}$ ). The VAT volume (3.45 vs. 2.53 L,  $p = 3.12 \times 10^{-12}$ ) and VAT area (190.82 vs. 148.71 cm<sup>2</sup>,  $p = 1.01 \times 10^{-10}$ ), as well as SAT volume

(5.43 vs. 4.47 L,  $p = 7.39 \times 10^{-7}$ ) and SAT area (297.76 vs. 258.06 cm<sup>2</sup>,  $p = 2.83 \times 10^{-5}$ ) were greater in diabetic patients. VSR was higher in patients with type 2 diabetes (0.62 vs. 0.55,  $p = 1.69 \times 10^{-3}$ ).

These trends generally held when stratifying by sex (Figure S3), as women with diabetes showed significantly higher SHAD (−4.99 vs. −7.97 HU,  $p = 8.62 \times 10^{-5}$ ), VSR (0.43 vs. 0.36,  $p = 3.41 \times 10^{-4}$ ), VAT (2.66 vs. 2.01 L,  $p = 1.92 \times 10^{-8}$ ), SAT (6.23 vs. 5.16 L,  $p = 9.14 \times 10^{-4}$ ) and LV (1.57 vs. 1.42 L,  $p = 2.44 \times 10^{-6}$ ) than women without diabetes, and men with diabetes showed significantly higher SHAD (−4.15 vs. −5.64 HU,  $p = 1.61 \times 10^{-4}$ ), VAT (4.37 vs. 3.46 L,  $p = 8.32 \times 10^{-7}$ ), SAT (4.98 vs. 3.81 L,  $p = 2.63 \times 10^{-5}$ ) and LV (1.87 vs. 1.74 L,  $p = 1.92 \times 10^{-3}$ ) than men without diabetes. However, VSR values between diabetic and nondiabetic males, as well as SV values between diabetic and nondiabetic males and females were nonsignificant. Between the sexes, median SHAD (−4.15 vs. −4.99 HU,  $p = 4.05 \times 10^{-1}$ ), VSR (0.93 vs. 0.43,  $p < 2.2 \times 10^{-16}$ ), VAT (4.37 vs. 2.66 L,  $p < 2.2 \times 10^{-16}$ ), LV (1.87 vs. 1.57 L,  $p = 3.84 \times 10^{-9}$ ) and SV (0.23 vs. 0.16 L,  $p = 3.82 \times 10^{-11}$ ) were significantly higher among male diabetics, while abdominal SAT (6.23 vs. 4.98 L,  $p = 9.55 \times 10^{-8}$ ) volume was significantly higher in female diabetics.

### 3.2 | Multivariate analysis

The multivariate analyses examined ORs of hepatic and abdominal IDPs with type 2 diabetes presence, controlling for age, sex, race and

Total (n = 1594)	Nondiabetic (n = 950)	T2DM (n = 644)	p-Value
Hepatic IDP values			
LMA (HU)	50.9 [44.0, 56.6]	47.0 [39.3, 54.3]	$1.36 \times 10^{-10}$
SMA (HU)	44.3 [39.1, 48.0]	43.2 [37.6, 47.8]	$2.67 \times 10^{-2}$
SHAD (HU)	−6.88 [−12.0, −1.47]	−4.49 [−10.1, 2.53]	$1.34 \times 10^{-8}$
HS prevalence (n [%])	263 (27.7)	269 (41.8)	$4.85 \times 10^{-9}$
LV (L)	1.58 [1.30, 1.94]	1.74 [1.41, 2.12]	$5.02 \times 10^{-8}$
SV (L)	0.18 [0.12, 0.26]	0.19 [0.12, 0.28]	$2.67 \times 10^{-2}$
Abdominal fat IDP values			
VAT volume (L)	2.53 [1.33, 4.06]	3.45 [2.04, 5.02]	$3.12 \times 10^{-12}$
SAT volume (L)	4.47 [2.78, 7.15]	5.43 [3.54, 7.83]	$7.39 \times 10^{-7}$
VAT area (cm <sup>2</sup> )	148.71 [91.26, 227.26]	190.82 [124.16, 272.0]	$1.01 \times 10^{-10}$
SAT area (cm <sup>2</sup> )	258.06 [175.08, 390.40]	297.76 [207.92, 428.26]	$2.83 \times 10^{-5}$
VSR	0.55 [0.34, 0.89]	0.62 [0.39, 0.97]	$1.69 \times 10^{-3}$

**TABLE 2** Imaging derived phenotype (IDP) values using computed tomography from the patient cohort.

Note: LV, SV, SMA, LMA, SHAD, VAT, SAT and VSR are arranged as median [Q1, Q3]. HS prevalence for each group is formatted as sample size (percentage), where SHAD  $\geq -1$  HU or LMA  $< 40$  HU is classified as a HS diagnosis. p-Values were calculated using a Wilcoxon rank-sum test to determine statistically significant differences between the 'Nondiabetic' and 'T2DM' groups and were corrected using Benjamini-Hochberg false discovery rate correction for multiple testing.

Abbreviations: HS, hepatic steatosis; HU, Hounsfield unit; LMA, liver mean attenuation value; LV, liver volume; SAT, subcutaneous adipose tissue; SHAD, spleen-hepatic attenuation difference; SMA, spleen mean attenuation value; SV, spleen volume; T2DM, type 2 diabetes mellitus; VAT, visceral adipose tissue; VSR, visceral-to-subcutaneous fat volume ratio.

BMI (Table 3). When examining the IDPs specifically, all except abdominal SAT were independently associated with diabetes: SHAD (OR 1.04, 95% CI [1.02–1.05]); LV (OR 1.63, 95% CI [1.31–2.04]); SV (OR 4.53, 95% CI [1.89–10.99]); VAT (OR 1.24, 95% CI [1.17–1.33]); and VSR (OR 2.87, 95% CI [1.96–4.20]).

The analysis using the combined model for multiple abdominal IDPs (Figure S4) yielded independent associations for SHAD (OR 1.03, 95% CI [1.02–1.04]), LV (OR 1.36, 95% CI [1.07–1.74]) and VSR (OR 2.36, 95% CI [1.60–3.49]). SV was no longer independently associated with type 2 diabetes presence after controlling for hepatic and abdominal fat distribution IDPs (OR 1.86, 95% CI [0.70–4.90]). When the continuous predictors in the model were standardised, VSR (OR 1.40, 95% CI [1.20–1.63]) exhibited a larger association with diabetes presence than BMI, LV, SV and SHAD.

Even after removing BMI from the multivariate analyses (Figure S5), all of the IDPs were associated with diabetes: SHAD (OR 1.04, 95% CI [1.03–1.05]); LV (OR 1.80, 95% CI [1.47–2.20]); SV (OR 6.36, 95% CI [2.71–15.12]); VAT (OR 1.24, 95% CI [1.17–1.30]); SAT (OR 1.06, 95% CI [1.03–1.10]); and VSR (OR 2.73, 95% CI [1.87–3.99]).

#### 4 | DISCUSSION

In this study, we applied an automated machine learning algorithm to imaging and clinical data from a tertiary-care academic biobank to characterise hepatic and abdominal adiposity patterns in patients with and without type 2 diabetes. Our results demonstrate robust associations on CT scans between various metrics associated with abdominal obesity-related features, including HS, hepatosplenomegaly and the overall distribution of abdominal adipose tissue, with the presence of type 2 diabetes. Prior studies have examined the relationship of individual image-derived abdominal adipose values with type 2 diabetes, which limits the ability to compare the relative contribution of different fat compartments or organ characteristics to disease presence.<sup>14–16,18</sup> Our study uses an integrative approach to simultaneously evaluate these abdominal IDPs on a large-scale basis, which enables a comprehensive assessment of metabolic imaging features and their relative contributions to the presence of type 2 diabetes.

Among abdominal adiposity values, abdominal VAT and VSR have the strongest associations with type 2 diabetes presence, holding BMI constant. Because BMI does not delineate body fat distribution and muscle mass,<sup>32,33</sup> VSR and VAT may serve as alternative metrics for obesity and better reflect the relationship of abdominal obesity to type 2 diabetes.<sup>34–37</sup> VSR exhibited a stronger association with type 2 diabetes presence than BMI in the standardised combined regression, which supports the notion that fat distribution conveys information beyond overall adiposity.<sup>38,39</sup> Even after removing BMI from the regression, VSR still has an independent association with diabetes, suggesting that VSR captures a unique aspect of type 2 diabetes.<sup>40</sup> In contrast, abdominal SAT volume was not associated with diabetes presence in models with BMI adjustment; however, the association was observed after BMI was excluded from the model, likely reflecting

**TABLE 3** Odds ratio model of type 2 diabetes presence against abdominal adipose imaging phenotype values and demographic characteristics.

Variables	Specific IDP variables											
	IDP: SHAD		IDP: LV		IDP: SV		IDP: VAT		IDP: SAT		IDP: VSR	
	OR (95% CI)	p-Value	OR (95% CI)	p-Value	OR (95% CI)	p-Value	OR (95% CI)	p-Value	OR (95% CI)	p-Value	OR (95% CI)	p-Value
Age	1.01 (1.00–1.02)	7.21 × 10 <sup>-2</sup>	1.01 (1.00–1.02)	2.59 × 10 <sup>-2</sup>	1.01 (1.00–1.02)	2.82 × 10 <sup>-2</sup>	1.00 (0.99–1.01)	0.72	1.01 (1.00–1.02)	0.13	1.00 (0.99–1.01)	0.80
Sex <sup>a</sup>												
Male	1.24 (1.00–1.53)	7.21 × 10 <sup>-2</sup>	1.09 (0.87–1.37)	0.52	1.18 (0.95–1.47)	0.18	0.87 (0.68–1.11)	0.43	1.31 (1.06–1.63)	3.47 × 10 <sup>-2</sup>	0.81 (0.62–1.07)	0.20
Race/ethnicity <sup>a</sup>												
Black	1.97 (1.56–2.48)	3.76 × 10 <sup>-8</sup>	1.97 (1.57–2.49)	6.58 × 10 <sup>-8</sup>	2.11 (1.66–2.69)	1.84 × 10 <sup>-8</sup>	2.28 (1.80–2.90)	6.18 × 10 <sup>-11</sup>	1.82 (1.45–2.29)	1.77 × 10 <sup>-6</sup>	2.26 (1.77–2.88)	3.46 × 10 <sup>-10</sup>
Asian/PI	2.57 (1.31–5.07)	1.21 × 10 <sup>-2</sup>	2.96 (1.51–5.82)	4.01 × 10 <sup>-3</sup>	2.79 (1.43–5.49)	5.14 × 10 <sup>-3</sup>	2.51 (1.28–4.94)	1.92 × 10 <sup>-2</sup>	2.48 (1.18–4.86)	2.83 × 10 <sup>-2</sup>	2.49 (1.27–4.90)	1.52 × 10 <sup>-2</sup>
Hispanic/Latino	1.60 (0.80–3.13)	0.20	1.34 (0.58–3.24)	0.31	1.41 (0.61–3.39)	0.18	1.46 (0.63–3.55)	0.31	1.32 (0.57–3.16)	0.32	1.46 (0.63–3.52)	0.20
Other	1.37 (0.69–2.66)	0.35	1.22 (0.61–2.35)	0.56	1.22 (0.61–2.35)	0.57	1.24 (0.62–2.42)	0.72	1.18 (0.60–2.27)	0.62	1.28 (0.64–2.48)	0.55
BMI	1.03 (1.01–1.04)	8.78 × 10 <sup>-4</sup>	1.02 (1.00–1.03)	7.66 × 10 <sup>-2</sup>	1.03 (1.01–1.04)	2.40 × 10 <sup>-3</sup>	1.00 (0.98–1.01)	0.72	1.02 (1.00–1.05)	5.69 × 10 <sup>-2</sup>	1.03 (1.02–1.05)	2.29 × 10 <sup>-5</sup>
IDP (see column headers)	1.04 (1.02–1.05)	8.72 × 10 <sup>-9</sup>	1.63 (1.31–2.04)	6.55 × 10 <sup>-5</sup>	4.53 (1.89–10.99)	2.40 × 10 <sup>-3</sup>	1.24 (1.17–1.33)	6.18 × 10 <sup>-11</sup>	1.02 (0.97–1.07)	0.51	2.87 (1.96–4.20)	2.32 × 10 <sup>-7</sup>

Note: Six iterations of logistic regressions (derived from Model 1) were performed, with different IDPs each time that are listed in the column headers. *p*-Values were adjusted with Benjamini–Hochberg (false discovery rate) correction with the statistical significance threshold *p* < 0.05.  
 Abbreviations: BMI, body mass index; CI, confidence interval; IDP, image-derived phenotype; LV, liver volume; SAT, abdominal subcutaneous adipose tissue volume; VSR, visceral-to-subcutaneous fat ratio.  
<sup>a</sup>The baseline category for the sex variable was female and for the race variable was White.

collinearity between BMI and abdominal SAT volume. Previous studies have found that SAT's relationship with diabetes is nuanced, with some evidence indicating that the specific location of SAT may even provide some protective effect against development of the disease.<sup>36,41,42</sup> Further research is necessary to comprehend the complex relationship between abdominal SAT and diabetes.

Hepatic steatosis, quantified through SHAD, was also strongly associated with diabetes presence in our cohort.<sup>43</sup> While a SHAD of 10 HU is widely used by radiologists as the cutoff for moderate-to-severe HS,  $-1$  HU has been histologically proven to coincide with at least mild steatotic liver disease.<sup>31</sup> By redefining the parameters of HS to make it more sensitive, we captured a larger proportion of patients with more mild degrees of HS and showed its association with type 2 diabetes. Moreover, the observed associations between diabetes and increased liver and SVs highlight how metabolic dysfunction and fatty infiltration can manifest as detectable structural organ changes on imaging.<sup>16,18</sup> The relationship between SV and type 2 diabetes has been relatively understudied<sup>18,19</sup>; here we demonstrate that SV is independently correlated with type 2 diabetes presence on CT, but the effect does not persist after controlling for hepatic and abdominal adiposity. Prior MRI-based studies have found larger SVs in type 2 diabetes patients, but SV is not independently associated with the disease after controlling for liver-related factors, supporting the interpretation that splenic changes are secondary to hepatic manifestations rather than directly interconnected to type 2 diabetes.<sup>44,45</sup>

Beyond these associations, the methodology used in this study has important implications for clinical research. Opportunistic and automated analysis of CT imaging allows for the large-scale extraction of metabolic risk factors without presenting additional cost, time for manual quantification or patient burden.<sup>8,12</sup> Prior CT-based studies have quantified various data such as bone mineral density, aortic calcium and skeletal muscle mass to predict metabolic syndromes and cardiovascular disease.<sup>46-48</sup> By combining EHR clinical data, such IDPs may support population-level type 2 diabetes risk stratification and enable future studies to predict disease progression or incident diabetes.<sup>47,49,50</sup>

This study has several strengths, such as the racial diversity of the PMBB patient population, although some racial cohorts had small sample sizes (such as Asian/Pacific Islander and Hispanic/Latino). Also, the biobank data is taken from patients who have diseases, whereas the UK Biobank consists mainly of healthy participants.<sup>51</sup> While the biobank's patient data is skewed to the geographic and demographic characteristics of southeastern Pennsylvania and New Jersey,<sup>52</sup> it does include patients from multiple hospitals and clinics in urban, suburban and rural settings. A limitation of this study was the use of one CT scan to be representative of the patient. Although we could define associations between adiposity and diabetes, given the study's cross-sectional design, we were unable to determine a causal relationship of these IDPs to the onset of diabetes or track disease pathogenesis across CT scan dates. Lastly, the use of phecodes to infer certain conditions presented some challenges since phecodes can imperfectly distinguish or group certain phenotypes.<sup>53</sup> The use of HbA1c values within 1 year of the abdominal CT scan to define diabetes status,

rather than phecodes, improves temporal relevance as phecodes may reflect historical diagnoses or incomplete coding at the date of CT acquisition. Multi-centre observational longitudinal studies that examine abdominal IDPs over consecutive abdominal CT scans can provide insight into how hepatic and abdominal fat distribution changes influence diabetes progression.

In future research, we hope to further elucidate the relationship between diabetes incidence, HS and abdominal fat distribution. A Korean study determined the VSR cutoff for men and women for predicting the incidence of type 2 diabetes, but no study has been done yet in America, which is more heterogeneous.<sup>35,40</sup> VSR holds promise as a metric to more accurately describe abdominal obesity and adiposity, and we hope to see it calculated and employed within clinical practice soon. Moreover, incorporation of the nutritional data of this patient population can provide insight into how diet and dietary modifications influence abdominal adiposity and disease aetiology.<sup>54</sup> Current research is underway to explore how diet can cause changes in imaging before clinical manifestations occur.<sup>55</sup>

In summary, HS, obesity and diabetes are interlinked findings, and their mild presentations potentially can serve as harbingers for more severe, even life-threatening disease.<sup>1,3,38</sup> By applying artificial intelligence and using EHR data to characterise the relationship of IDPs with diabetes, we have confirmed and established novel associations that serve as a high-level overview to encourage future inquiry into how adiposity is related to diabetes mellitus. This study presents a scalable framework for the use of machine learning to capture IDPs in a diabetic population to catalyse translational science.

## AUTHOR CONTRIBUTIONS

**RHT:** Conceptualisation, methodology, validation, formal analysis, investigation, data curation, writing—original draft, writing—review and editing, visualisation. **PR:** Conceptualisation, methodology, software, validation, formal analysis, investigation, data curation, writing—review and editing, visualisation. **MH:** Conceptualisation, methodology, formal analysis, investigation, data curation. **ET:** Conceptualisation, methodology, software, formal analysis, investigation, data curation. **SS:** Methodology, validation, investigation. **ABh:** Methodology, validation, investigation. **MM:** Methodology, software, validation, formal analysis, investigation, data curation. **JTD:** Methodology, software, validation, formal analysis, investigation, data curation. **JG:** Methodology, resources, data curation. **CK:** Methodology, validation, investigation. **DJR:** Resources, data curation. **ABo:** Methodology, validation, investigation. **WRW:** Conceptualisation, methodology, investigation, resources, data curation, writing—review and editing, supervision. **HS:** Conceptualisation, methodology, investigation, resources, data curation, writing—review and editing, visualisation, supervision.

## ACKNOWLEDGEMENTS

We acknowledge the Penn Medicine BioBank (PMBB) for providing data and thank the patient-participants of Penn Medicine who consented to participate in this research programme. The Institutional Review Board of the University of Pennsylvania approved the PMBB (IRB 808346, IRB 813913 and IRB 817977).

## FUNDING INFORMATION

Walter R. Witschey is supported by National Institutes of Health (NIH) National Heart, Lung, and Blood Institute (NHLBI) grants R01HL171709 and R01HL169378 and NIH National Institute of Biomedical Imaging and Bioengineering (NIBIB) grant P41EB029460. Hersh Sagreiya was supported by a Radiological Society of North America Research Scholar Grant #RSCH2028 and was supported in part by the Institute for Translational Medicine and Therapeutics' (ITMAT) Transdisciplinary Program in Translational Medicine and Therapeutics. Walter R. Witschey, Hersh Sagreiya, James Gee, and Jeffrey T. Duda were supported by the NIH Office of the Director grant OT2OD038048. Walter R. Witschey and Hersh Sagreiya were supported by NIH NIBIB grant R21EB036734. The PMBB is supported by the Perelman School of Medicine at the University of Pennsylvania, a gift from the Smilow family, and the National Center for Advancing Translational Sciences of the National Institutes of Health under CTSA award number UL1TR001878. The content is solely the responsibility of the authors and does not represent the views of the Department of Veterans Affairs, the National Institutes of Health, or the United States Government. Matthew MacLean received funding from the Sarnoff Cardiovascular Research Foundation.

## CONFLICT OF INTEREST STATEMENT

The authors declare no competing interests.

## PEER REVIEW

The peer review history for this article is available at <https://www.webofscience.com/api/gateway/wos/peer-review/10.1111/dom.70557>.

## DATA AVAILABILITY STATEMENT

The data that support the findings of this study are available from the corresponding author upon reasonable request.

## ORCID

Richard H. Tran  <https://orcid.org/0009-0005-1466-9252>

## REFERENCES

- Sun H, Saeedi P, Karuranga S, Pinkepank M, et al. IDF Diabetes Atlas: global, regional and country-level diabetes prevalence estimates for 2021 and projections for 2045. *Diabetes Res Clin Pract.* 2022;183:109119.
- Mobasser M, Shirmohammadi M, Amiri T, Vahed N, Hosseini Fard H, Ghojzadeh M. Prevalence and incidence of type 1 diabetes in the world: a systematic review and meta-analysis. *Health Promot Perspect.* 2020;10(2):98-115.
- Alva ML, Chakkalakal RJ, Moin T, Galaviz KI. The diabetes prevention gap and opportunities to increase participation in effective interventions. *Health Aff Millwood.* 2022;41(7):971-979.
- Kaul P, Chu LM, Dover DC, Yeung RO, Eurich DT, Butalia S. Disparities in adherence to diabetes screening guidelines among males and females in a universal care setting: a population-based study of 1,380,697 adults. *Lancet Reg Health.* 2022;14:100320.
- Gopalan A, Mishra P, Alexeeff SE, et al. Prevalence and predictors of delayed clinical diagnosis of type 2 diabetes: a longitudinal cohort study. *Diabet Med.* 2018;35(12):1655-1662.
- Pyrros A, Borstelmann SM, Mantravadi R, et al. Opportunistic detection of type 2 diabetes using deep learning from frontal chest radiographs. *Nat Commun.* 2023;14(1):4039.
- Dunne CL, Elzinga JL, Vorobeichik A, et al. A systematic review of interventions to reduce computed tomography usage in the emergency department. *Ann Emerg Med.* 2022;80(6):548-560.
- Chae A, Yao MS, Sagreiya H, et al. Strategies for implementing machine learning algorithms in the clinical practice of radiology. *Radiology.* 2024;310(1):e223170.
- Bentley P, Ganesalingam J, Carlton Jones AL, et al. Prediction of stroke thrombolysis outcome using CT brain machine learning. *NeuroImage: Clin.* 2014;4:635-640.
- Sebro R, la De Garza-Ramos C. Machine learning for the prediction of osteopenia/osteoporosis using the CT attenuation of multiple osseous sites from chest CT. *Eur J Radiol.* 2022;155:110474.
- Vu PT, Chahine C, Chatterjee N, et al. CT imaging-derived phenotypes for abdominal muscle and their association with age and sex in a medical biobank. *Sci Rep.* 2024;14(1):14807.
- Khalifa M, Albadawy M. AI in diagnostic imaging: revolutionising accuracy and efficiency. *Comput Methods Programs Biomed Update.* 2024;5:100146.
- Song I, Thompson EW, Verma A, et al. Clinical correlates of CT imaging-derived phenotypes among lean and overweight patients with hepatic steatosis. *Sci Rep.* 2024;14(1):53.
- Zeb I, Li D, Nasir K, Katz R, Larijani VN, Budoff MJ. Computed tomography scans in the evaluation of fatty liver disease in a population based study: the multi-ethnic study of atherosclerosis. *Acad Radiol.* 2012;19(7):811-818.
- MacLean MT, Jehangir Q, Vujkovic M, et al. Quantification of abdominal fat from computed tomography using deep learning and its association with electronic health records in an academic biobank. *J Am Med Inform Assoc.* 2021;28(6):1178-1187.
- Tallam H, Elton DC, Lee S, Wakim P, Pickhardt PJ, Summers RM. Fully automated abdominal CT biomarkers for type 2 diabetes using deep learning. *Radiology.* 2022;304(1):85-95.
- Yao MS, Chae A, MacLean MT, et al. SynthA1c: towards clinically interpretable patient representations for diabetes risk stratification. *Predict Intell Med.* 2023;14277:46-57.
- Henderson JM, Heymsfield SB, Horowitz J, Kutner MH. Measurement of liver and spleen volume by computed tomography. Assessment of reproducibility and changes found following a selective distal splenorenal shunt. *Radiology.* 1981;141(2):525-527.
- Tsushima Y, Endo K. Spleen enlargement in patients with nonalcoholic fatty liver: correlation between degree of fatty infiltration in liver and size of spleen. *Dig Dis Sci.* 2000;45(1):196-200.
- Davidson LE, Kelley DE, Heshka S, et al. Skeletal muscle and organ masses differ in overweight adults with type 2 diabetes. *J Appl Physiol.* 2014;117(4):377-382.
- Wells MM, Li Z, Addeman B, et al. Computed tomography measurement of hepatic steatosis: prevalence of hepatic steatosis in a Canadian population. *Can J Gastroenterol Hepatol.* 2016;2016:4930987.
- Wan Y, Wang D, Li H, Xu Y. The imaging techniques and diagnostic performance of ultrasound, CT, and MRI in detecting liver steatosis and fat quantification: a systematic review. *J Radiat Res Appl Sci.* 2023;16(4):100658.
- Vernuccio F, Cannella R, Bartolotta TV, Galia M, Tang A, Brancatelli G. Advances in liver US, CT, and MRI: moving toward the future. *Eur Radiol Exp.* 2021;5(1):52.
- Neeland IJ, Yokoo T, Leinhard OD, Lavie CJ. 21st century advances in multimodality imaging of obesity for care of the cardiovascular patient. *JACC Cardiovasc Imaging.* 2021;14(2):482-494.
- Denny JC, Bastarache L, Ritchie MD, et al. Systematic comparison of phenome-wide association study of electronic medical record data and genome-wide association study data. *Nat Biotechnol.* 2013;31(12):1102-1110.

26. Joseph JJ, Ortiz R, Acharya T, Golden SH, López L, Deedwania P. Cardiovascular impact of race and ethnicity in patients with diabetes and obesity: JACC focus seminar 2/9. *J Am Coll Cardiol*. 2021;78(24):2471-2482.
27. Caleyachetty R, Barber TM, Mohammed NI, et al. Ethnicity-specific BMI cutoffs for obesity based on type 2 diabetes risk in England: a population-based cohort study. *Lancet Diabetes Endocrinol*. 2021;9(7):419-426.
28. Park J, MacLean MT, Lucas AM, et al. Exome-wide association analysis of CT imaging-derived hepatic fat in a medical biobank. *Cell Rep Med*. 2022;3(12):100855.
29. MacLean MT, Jehangir Q, Vujkovic M, et al. Linking abdominal imaging traits to electronic health record phenotypes. medRxiv. 2020. doi: [10.1101/2020.09.08.20190330](https://doi.org/10.1101/2020.09.08.20190330)
30. Haghshomar M, Antonacci D, Smith AD, Thaker S, Miller FH, Borhani AA. Diagnostic accuracy of CT for the detection of hepatic steatosis: a systematic review and meta-analysis. *Radiology*. 2024;313(2):e241171.
31. Park YS, Park SH, Lee SS, et al. Biopsy-proven nonsteatotic liver in adults: estimation of reference range for difference in attenuation between the liver and the spleen at nonenhanced CT. *Radiology*. 2011;258(3):760-766.
32. Freemantle N, Holmes J, Hockey A, Kumar S. How strong is the association between abdominal obesity and the incidence of type 2 diabetes? *Int J Clin Pract*. 2008;62(9):1391-1396.
33. Piche ME, Tchernof A, Despres JP. Obesity phenotypes, diabetes, and cardiovascular diseases. *Circ Res*. 2020;126(11):1477-1500.
34. Kaess BM, Pedley A, Massaro JM, Murabito J, Hoffmann U, Fox CS. The ratio of visceral to subcutaneous fat, a metric of body fat distribution, is a unique correlate of cardiometabolic risk. *Diabetologia*. 2012;55(10):2622-2630.
35. Kim EH, Kim H-K, Lee MJ, et al. Sex differences of visceral fat area and visceral-to-subcutaneous fat ratio for the risk of incident type 2 diabetes mellitus. *Diabetes Metab J*. 2022;46(3):486-498.
36. Neeland IJ, Ayers CR, Rohatgi AK, et al. Associations of visceral and abdominal subcutaneous adipose tissue with markers of cardiac and metabolic risk in obese adults. *Obesity*. 2013;21(9):E439-E447.
37. Smith JD, Borel A-L, Nazare J-A, et al. Visceral adipose tissue indicates the severity of cardiometabolic risk in patients with and without type 2 diabetes: results from the INSPIRE ME IAA study. *J Clin Endocrinol Metab*. 2012;97(5):1517-1525.
38. Linge J, Cariou B, Neeland IJ, Petersson M, Rodríguez Á, Leinhard OD. Skewness in body fat distribution pattern links to specific cardiometabolic disease risk profiles. *J Clin Endocrinol Metab*. 2024;109(3):783-791.
39. Wang D, Morton JI, Magliano DJ, Shaw JE. Comparison of subcutaneous, visceral, liver and muscle fat depots in relation to prevalent and incident diabetes. *Diabetes Obes Metab*. 2025;27(11):6304-6313.
40. Oh YH, Moon JH, Kim HJ, Kong MH. Visceral-to-subcutaneous fat ratio as a predictor of the multiple metabolic risk factors for subjects with normal waist circumference in Korea. *Diabetes Metab Syndr Obes*. 2017;10:505-511.
41. Golan R, Shelef I, Rudich A, et al. Abdominal superficial subcutaneous fat: a putative distinct protective fat subdepot in type 2 diabetes. *Diabetes Care*. 2012;35(3):640-647.
42. Foster MT, Softic S, Caldwell J, Kohli R, deKloet AD, Seeley RJ. Subcutaneous adipose tissue transplantation in diet-induced obese mice attenuates metabolic dysregulation while removal exacerbates it. *Physiol Rep*. 2013;1(2):e00015.
43. Richard J, Lingvay I. Hepatic steatosis and type 2 diabetes: current and future treatment considerations. *Expert Rev Cardiovasc Ther*. 2011;9(3):321-328.
44. Helgesson S, Tarai S, Langner T, et al. Spleen volume is independently associated with non-alcoholic fatty liver disease, liver volume and liver fibrosis. *Heliyon*. 2024;10(8):e28123.
45. Soresi M, Giannitrapani L, Noto D, et al. Effects of steatosis on hepatic hemodynamics in patients with metabolic syndrome. *Ultrasound Med Biol*. 2015;41(6):1545-1552.
46. Kullberg J, Hedström A, Brandberg J, et al. Automated analysis of liver fat, muscle and adipose tissue distribution from CT suitable for large-scale studies. *Sci Rep*. 2017;7(1):10425.
47. Zambrano Chaves JM, Wentland AL, Desai AD, et al. Opportunistic assessment of ischemic heart disease risk using abdominopelvic computed tomography and medical record data: a multimodal explainable artificial intelligence approach. *Sci Rep*. 2023;13(1):21034.
48. Magudia K, Bridge CP, Bay CP, et al. Utility of normalized body composition areas, derived from outpatient abdominal CT using a fully automated deep learning method, for predicting subsequent cardiovascular events. *AJR Am J Roentgenol*. 2023;220(2):236-244.
49. Pickhardt PJ, Graffy PM, Perez AA, Lubner MG, Elton DC, Summers RM. Opportunistic screening at abdominal CT: use of automated body composition biomarkers for added cardiometabolic value. *Radiographics*. 2021;41(2):524-542.
50. Pickhardt PJ, Graffy PM, Zea R, et al. Utilizing fully automated abdominal CT-based biomarkers for opportunistic screening for metabolic syndrome in adults without symptoms. *AJR Am J Roentgenol*. 2021;216(1):85-92.
51. Verma A, Damrauer SM, Naseer N, et al. The Penn Medicine BioBank: towards a genomics-enabled learning healthcare system to accelerate precision medicine in a diverse population. *J Pers Med*. 2022;12(12):1974.
52. Prictor M, Teare HJA, Kaye J. Equitable participation in biobanks: the risks and benefits of a "dynamic consent" approach. *Front Public Health*. 2018;6:253.
53. Bastarache L. Using Phecodes for research with the electronic health record: from PheWAS to PheRS. *Annu Rev Biomed Data Sci*. 2021;4:1-19.
54. Mollard RC, Sénéchal M, MacIntosh AC, et al. Dietary determinants of hepatic steatosis and visceral adiposity in overweight and obese youth at risk of type 2 diabetes. *Am J Clin Nutr*. 2014;99(4):804-812.
55. Compher CW, Quinn R, Haslam R, et al. Penn healthy diet survey: pilot validation and scoring. *Br J Nutr*. 2024;131(1):156-162.

## SUPPORTING INFORMATION

Additional supporting information can be found online in the Supporting Information section at the end of this article.

**How to cite this article:** Tran RH, Raghupathy P, Hazim M, et al. Hepatic and abdominal adiposity in type 2 diabetes as assessed with machine learning on computed tomography scans. *Diabetes Obes Metab*. 2026;1-10. doi:[10.1111/dom.70557](https://doi.org/10.1111/dom.70557)